

UNIVERSITY OF LATVIA
INSTITUTE OF SOLID STATE PHYSICS



UGIS GERTNERS

**PHOTO INDUCED SURFACE MODULATION IN
AMORPHOUS CHALCOGENIDES**

SUMMARY OF DOCTORAL THESIS

Submitted for the degree of Doctor of Physics

Subfield of Solid State Physics

Riga, 2015

University of Latvia
Institute of Solid State Physics

Ugis Gertners

PHOTO INDUCED SURFACE MODULATION IN
AMORPHOUS CHALCOGENIDES

Summary of Doctoral Thesis

Submitted for the degree of Doctor of Physics
Subfield of Solid State Physics

Riga, 2015

The doctoral thesis was carried out at the Institute of Solid State Physics of University of Latvia from 2010 to 2014.



This work has been supported by the European Social Fund within the project «Support for Doctoral Studies at University of Latvia».

The work contains the introduction, three chapters, conclusions, thesis and reference list.

Form of the thesis: dissertation in physics, subfield of solid state physics.

Supervisor:

Dr. phys. Jānis Teteris, senior researcher, Institute of Solid State Physics, University of Latvia.

Reviewers:

- 1) *Dr. habil. phys. Andrejs Cēbers*, professor, University of Latvia;
- 2) *Dr. habil. phys. Andris Ozols*, professor, Riga Technical University;
- 3) *Dr. phys. Vjačeslavs Gerbreders*, senior researcher, Innovative Microscopy Centre, Daugavpils University;

The thesis will be defended at the public session of the specialized Doctoral Committee of physics, astronomy and mechanics, University of Latvia, at 15:00 on April 17, 2015 in the conference hall of the Institute of Solid State Physics at 8 Kengaraga street.

The thesis is available at the Library of the University of Latvia, Raina blvd. 19.

This thesis is accepted for the commencement of the degree of Doctor of Physics by the specialized Doctoral Committee of physics, astronomy and mechanics, University of Latvia.

Chairman of the specialized Doctoral Committee *Dr. phys. Uldis Rogulis*
Secretary of the specialized Doctoral Committee **Laureta Buševica**

© University of Latvia, 2015
© Ugis Gertners, 2015

ISBN 978-9984-45-972-1

ABSTRACT

Amorphous chalcogenide semiconductors (As-S, As-Se, Ge-S, Ge-Se e.g.) thin films causes increasing interest as promising material for data optical recording and processing. Significant changes of photo-induced optical properties, such as the refractive index (Δn to 0.8), viscosity, micro hardness and bandgap changes (ΔE_g to 0.4eV) in these materials make it possible to perform phase as well as amplitude recording in thin films. Photo-induced changes in chalcogenide semiconductors are related to the transformation of chemical bonds, which determines the high resolution ($\sim 10^4 \text{ nm}^{-1}$) [1-3] of the material. The listed things are those that make amorphous chalcogenides as competitive materials for optical recording in holography, as well as in making optical elements of the surface relief in nanolithography, and also in data transmission and storage in information technology [4-5]. Recent studies have shown that soft material (such as amorphous chalcogenide) exposure to light forms a significant deformation [6], which is associated with the susceptibility to radiation. This process is reversible and the obtained deformation is not a density effect, because the entry can be deleted thermally - by heating [6], as well as optically - by illuminating the sample [7]. The dissertation is based on this phenomenon, which objective is to do a research on the amorphous chalcogenide susceptibility to light. As one of the research methods, a direct holographic record will be used, i.e., creating surface relief or holographic grating in chalcogenides directly during the recording without any additional processing, like etching. Complete development of this method opens wide range of usage possibilities in optical element production and utilization, as well as in introduction of new and innovative technologies. There is still a lot of interesting phenomena in amorphous chalcogenide that are not well understood and explained in a microscopic level [8-9] and so this work will be directly involved in the process of research. Record efficiency dependence from its parameters (intensity, polarization) and recording conditions will be examined, recording process in microscopic level will be explained. Optical properties for obtained nanostructures will be studied, such as transmission, reflection, diffraction efficiency, etc. The obtained structures will be viewed by atomic force microscopy, determining their shape and size.

TABLE OF CONTENTS

ABSTRACT	3
TABLE OF CONTENTS	4
INTRODUCTION	6
Motivation and Scientific Novelty of the Work	6
Aim and Objectives of the Work	7
Author's Contribution	7
1. LITERATURE REVIEW	9
2. EXPERIMENTAL	12
2.1. Studied Samples and Methods of Study	12
2.2. Research Methodology	12
3. RESULTS AND DISCUSSION	14
3.1. Direct record and its research with holographic methods	14
3.1.1. <i>Direct record in amorphous thin films</i>	15
3.1.2. <i>Computer visualizations of plain wave interference</i> ...	16
3.1.3. <i>Multi-beam holographic recording experiment comparison with theory</i>	18
3.1.4. <i>Chalcogenide photo-induced softening effect on direct holographic record</i>	18
3.1.5. <i>Polarization effect on holographic grid record and on supplemental beam</i>	20
3.1.6. <i>Theoretical polarization distribution for two-beam interference</i>	22
3.1.7. <i>Mass transfer direction during the holographic recording based on the foto-induced birefringence</i>	24
3. 2. Direct recording and its research after the sample irradiation through narrow slit	27
3.2.1. <i>Mass transfer direction</i>	27

3.2.2. <i>Development of the record in optical slit experiment in time</i>	28
3.2.3. <i>Overview of the optical slit experiments</i>	29
CONCLUSIONS	32
THESIS	33
REFERENCES	34
AUTOR'S PUBLICATION LIST	38
SCI Publications	38
Other Publications	38
PARTICIPATION IN CONFERENCES	40
ACKNOWLEDGEMENT	42

INTRODUCTION

Motivation and Scientific Novelty of the Work

Fast, reversible one-step direct surface structuring is open and is being actively investigated in various light sensitive materials, but its physical interpretation and a complete recording mechanism of the model is not yet fully understood [8-9]. A full research of this process provides a wide range of usage possibilities in different equipment, such as the nano/micro structuring of the surface, as well as ready-made components for machine composition. The obtained grating has already been demonstrated as an optical polarizers [10], angular or spectral filters [11-12], transition optical devices [13], in diffractometers, in spectrometers and other devices. Solutions are offered also for photonic crystals [14] and they are also used in the production of laser, where the wavelength is changed depending on the grating's geometrical parameters [15-16]. Direct recording equipment, of course, can also be used for data storage devices [17]. Fast, one-step direct holographic recording is offered as a solution to the instant holography design [18], which can certainly find a practical use in various fields. These are just a few of possible options that could be gained or what could be improved with the direct recording method, and that is why it's so important to continue this process of advanced research. Also, this dissertation is devoted to the advance research of direct recording possibilities of light sensitive amorphous chalcogenides. The novelty of this work's research includes the following articles:

- Displayed the erasing of direct holographic recording with the same recording equipment by moving the interference pattern by half of its period;
- Acquired multi-beam (three and four-beam) interferences or holographic recording intensity distribution over a wide range of polarized interfering light sources, as well as clearly displayed the acquisition process of given theoretical model;
- For the first time, there is acquired more detailed two-beam direct holographic recording efficiency dependence on supplemental beam as well as on intensity and polarization, and also dependence is acquired on recording beam polarizations with or without supplemental beam;
- Acquired detailed two-beam interference's or holographic recording intensity's and polarization distribution over a wide range of polarized interfering light sources and analyzed the polarization spectrum of a

given intensity distribution, as well as clearly displayed the acquisition process of given theoretical model;

- For the first time, explained the process of mass shifts during holographic recording based on material's photo-induced birefringence and diffraction efficiency correlations;
- For the first time, the mass-shift experiments are conducted using a rectangular light intensity gradient obtained from the narrow gap;
- Acquired detailed summary of rectangular light intensity gradient direct recording experiments at different gradient and/or supplemental beam polarizations, intensities and exposure durations.

Aim and Objectives of the Work

The aim is - advanced study of the changes of amorphous chalcogenide thin film mechanical and optical properties in the influence of optical radiation, focusing on radiation wavelength, intensity and polarization. In order to achieve the goal, it necessary to perform the following tasks:

1. Acquire amorphous chalcogenide (As-S, As-S-Se and Ge-Se) thin film with vacuum sputtering equipment;
2. Study the optical characteristics of the film and test its direct recording possibilities;
3. Theoretically and experimentally study multi-beam direct holographic recording possibilities in amorphous chalcogenides;
4. Study the direct holographic recording amorphous chalcogenide films, as well as study recording dependence on light intensity, polarization and photo-induced softening;
5. Determine the shape and size of acquired structures depending on various recording parameters;
6. Theoretically study the intensity and polarization distribution during the holographic recording and compare results with efficiency of grating record;
7. Determine the direction of mass drifts during holographic recording;
8. Study direct recording possibilities and directions of mass drift directions with a rectangular light intensity distribution at various light intensities, polarizations and record durations;

Author's Contribution

All the research were performed at the University of Latvia, Institute of Solid physics, Laboratory of Optical Recordings and Laboratory of Surface Physics. The author himself performed all of the experiments described in this dissertation, for example, recording of absorption spectrum, the direct holographic recording and direct optical gaps recording. Results of the experiment the author acquired in a wide range of variables (polarization, intensity, etc.), and also he has collected and studied the experimental data arrays. Work on atomic force microscope and high resolution optical microscope author has made at the Laboratory of Surface Physics. Theoretical calculations and acquired models of light and polarization distributions are also the author's work. The study analysis and conclusions author has made and discussed with his supervisor. The author has presented the results at international and local conferences. Most of the publication the author has written himself and submitted for publication in scientific journals.

1. LITERATURE REVIEW

Light and material interaction research process begins with the search of samples themselves and identifying laboratory capacity limits. The sample of research, being a holographic recording material, must be sufficiently light sensitive and with surface relief modulating potential during optical recording. All of such materials can be divided into two main categories: organic and inorganic materials. Inorganic materials have been selected in this work, more specifically, the amorphous chalcogenides. Chalcogenide semiconductors consist of the chalcogens of group VI elements (S, Se, Te) of Periodic Table covalently bonded with elements (P, As, Sb, Bi) in group V next to it and group IV elements (Si, Ge). They can be compounds of two, three or more elements, such as As-S, As-Se, As-S-Se, As-S-I, As-Te-Si-Ge, etc. Chalcogenides may be in both crystalline and amorphous state [1, 19].

Despite relatively large number of direct recording experimental results obtained for a whole range of inorganic materials (including amorphous chalcogenide semiconductors) [20-31] as well as a variety of light-sensitive organic azo molecule compounds [32-44], complete and comprehensive record microscopic model or mechanism is still not found. So far viscoelastic (or viscous mass flow) record model, directly not describing the microscopic forces, coincided very well with the experimentally observed results of the direct optical recording [45]. Later, the thickness of the film and velocity distribution inside the film was considered [46-47], which determined record's effectiveness in the model, or record's depth dependence on the film thickness. In the following improvement a photo-induced anisotropy was taken into account [48], which further described well anisotropic deformation in different experiments [49]. Finite elements' linear viscoelastic model also includes a finite compressibility [50], from which arises the fact that the surface tension acts as a counterforce to the surface relief formation, which in turn explains the saturation effect of the record. Finally, relief formation kinetics or nonlinear viscoelastic flow and deformation were obtained with lattice Monte Carlo simulation method [51-53]. No matter how good viscoelastic model would be, it does not give an idea of the forces involved and their nature, therefore, still there is an active research to determine the origins of microscopic forces inside the material.

The following will describe the most popular models, which perhaps describes the photo induced forces and their directions, which results in mass transfer in a specific direction. None of the following models are is

complete and comprehensive - each has its own deficiencies, which lead to the need for further advanced study of this process. Since the direct record relatively has been studied mainly in organic materials, these models too have been designed based on organic azo compounds, but they can also be generalized to all light-sensitive materials.

Asymmetric diffusion model

Simple anisotropic mass transfer mechanism was first described by Lefin and his colleagues in 1998 [54-55]. In this model, the mass transfer is observed in azo compounds under the influence of orientational concentration gradient. After random transfer principle molecules containing chromophores due to fast cycling between *trans* and *cis* states or in the result of isomerization mainly move to its greater axis direction. This process is described by the diffusion equation. Transfer probability is proportional to the molecular isomerization probability which, of course, depends on the light intensity and the angle between the molecular axis and the polarization direction of the light. This model provides the molecular flow away from the illuminated areas, which also coincides with the experimental results. However, contrary to that observed in experiments, asymmetric diffusion model provides the best results for small molecule compounds rather than polymers.

Mean-field model

The mechanism, which is based on electromagnetic forces, is quite promising, because it already contains radiation intensity and polarization. This model was first described by Pedersen and his colleagues in 1998 [56-57]. In organic azo compounds chromophores are in the potential created by neighboring chromophore dipole momentum. In the mean-field model chromophores are being oriented by light and in the result of uniformly oriented dipole attraction forces, chromophores are attracted to each other. Such model provides the mass transfer towards the light, therefore, obtained relief peaks will coincide with the light intensity peaks, which perform in liquid crystals, but not always perform experimentally in amorphous chalcogenides or amorphous polymers.

Permittivity (ϵ) gradient model

Model, based on the spatial modulation of permittivity ϵ was first described by Baldi in 2001 [58]. Here it is assumed that the spatially modulated refractive index is being induced in the film, which in turn is related to the spatially modulated permittivity. This assumption is fully justified, since most of the light-sensitive organic and inorganic materials

are characterized by photo-orientation and photo-induced birefringence. Electric field and permittivity gradient generates force:

$$\vec{f} = -\frac{\epsilon_0}{2} \vec{E}^2 \nabla \epsilon \quad 1-1$$

The given force is proportional to the permittivity gradient and electric field intensity towards the direction of mass transfer. It follows from the formula that the mass is transferred away from the permittivity gradient, which in most cases means that the mass transfers towards the unenlightened places. It follows from this model that any system with spatially modulated refractive index should be able to perform direct entries, although in literature there is nothing about it.

Electric field intensity gradient model

Kumar and colleagues introduced a mechanism based on the observation that the successful record requires an electric field component towards the direction of mass transfer [59-62]. Such a model can be described by the optical gradient force [63-64]. Spatial light modulation or modulation of electric field intensity and orientation leads to susceptibility χ modulation on the film surface. Electric field polarizes the material and the induced polarization is related to light intensity used and the local susceptibility χ :

$$\vec{P}_i = \epsilon_0 \chi \vec{E}_j, \quad 1-2$$

Where \vec{P}_i is polarization, and ϵ_0 is permittivity in vacuum, χ is susceptibility of the film, and \vec{E}_j is electric field created by light. Similar to electric field where dipole is affected by force, also in this case, forces appear from the light in polarized material. Force averaged in time has following appearance [61]:

$$\vec{f} = \langle (\vec{P} \cdot \nabla) \vec{E} \rangle \quad 1-3$$

From this formula we see that the record efficiency is connected to spatial modulation of susceptibility, electric field size and its gradient. Electric field intensity gradient force model includes mass transfer depending on the polarization of light, and thus describes well polarization dependence observed experimentally. However, different literature describes this force as insufficient for mass transfer in real system [50].

2. EXPERIMENTAL

2.1. Studied Samples and Methods of Study

Information was collected in the dissertation on amorphous chalcogenides which composition corresponds to formula As_2S_3 , $As_4S_{1.5}Se_{4.5}$ and $GeSe_3$. Photoresist with a film thickness of 1.7-3.3 μm were obtained with the method of condensation on the glass substrate by vacuum evaporation ($\sim 5 \times 10^{-5}$ Torr). Tantalum bowl was used as evaporator, in which the synthesized material was placed.

Film thickness and large surface relief period was determined by using profilometer *Veeco Dektak 150*. High resolution microscope NIKON ECLIPSE L150 and Veeco AFM CP-II atomic force microscope were used to assess visual characteristics of the film and to study surface topography, when taking micro-photos. Absorption spectrum of the film was determined in 250 - 800 nm range using Ocean Optic HR4000CG spectrometer.

2.3. Research Methodology

Dissertation consists of three parts, where the first part is devoted to thin films research used in the work. Absorption spectrum of the film will be determined, after which, lasers with a certain wavelength will be selected for direct recording research. We will make sure of the direct recording process reversibility by deleting record with fundamentally new technique. Record erasing option, in turn, suggests a physical mass transfer rather than a recording density or volume effect. Reversibility factor is a vital stage of the dissertation, because all the work further is based on the research of mass transfer processes in amorphous chalcogenides.

Second part will describe the direct or one-step (bypassing the chemical etching process) surface relief holographic recording and its effectiveness (principal scheme of the record Fig. 2.1a.). Grid formation process will be further examined, its characteristics, dependence of polarization and the softening of the sample. To reduce sample viscosity and increase its fluidity, independent light source will be used, which will illuminate the sample during the record. We will make sure about the selected essential effect of this additional illumination wavelength and polarization on the direct surface relief holographic recording. Mass transfer directions during the direct holographic recording will be determined based on the photo-induced birefringence. Plane wave

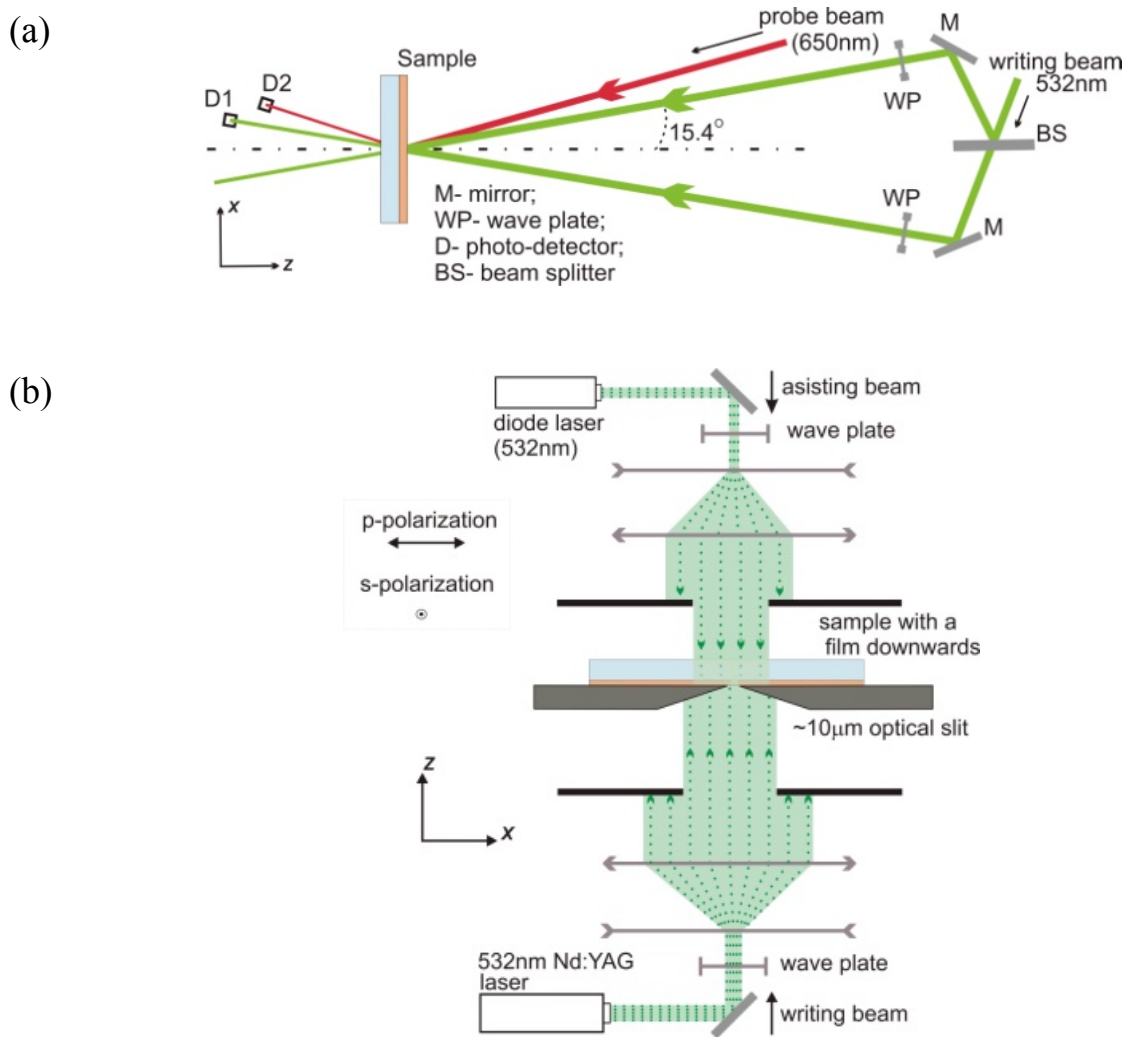


Fig. 2.1. Experimental setup for (a) direct holographic recording and (b) formation of surface-relief structures by illumination through an adjustable optical slit

interference intensity will be obtained, as well as the theoretical model of polarization modulation, which significantly will simplify the analysis of experimental data in this paragraph.

Third part will summarize the results of a rectangular light intensity distribution effects on the given sample (principal scheme of the record Fig. 2.1b.). Such type of light modulation will be provided by using a narrow, approximately 10μm wide optical slit. Given equipment with direct measurements allows determining the movement of direct recording, depending on any parameter, including intensity, polarization or exposure. The structure of recording equipment is very simple and is characterized by good resistance to vibration, laser intensity fluctuations and poor or non-existent coherence, which overall guarantees very precise and accurate results.

3. RESULTS AND DISCUSSION

3.1. Direct record and its research with holographic methods

In the typical surface relief (SRG) recording process (shown in Figure 3.1. and 3.2.) diffraction efficiency (DE) changes with time for amorphous chalcogenide semiconductor films. For this particular case recording was performed on As_2S_3 sample with p polarization ($I_1=I_2=0.2W/cm^2$). As the absorption and refractive index photo-induced changes in resist material are comparatively fast, transmission DE η_T (dashed curve) reaches maximum (~55% DE) very quickly. Due to overexposure the contrast of the volume grating decreases – η_T starts to decrease. At that time the reflection DE η_R (solid curve in Figure 3.1.) starts to increase linearly, which is an evidence of the surface-relief formation.

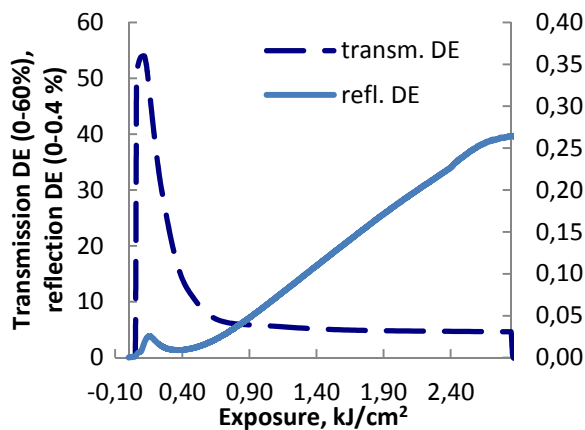


Fig. 3.1. Typical p polarization holographic record process depiction by taking transmission (650nm) and reflection (405nm) DE

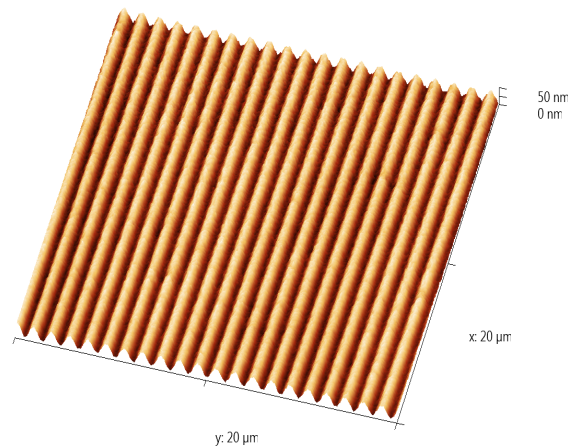


Fig. 3.2. Obtained hologram in amorphous As_2S_3 thin film, grating period $\Lambda=1\mu m$

From the literature and our experience we know that such direct recording process is reversible [7, 9]. Reversibility factor is a vital stage of the dissertation, because all the work further is based on the research of mass transfer processes in amorphous chalcogenides.

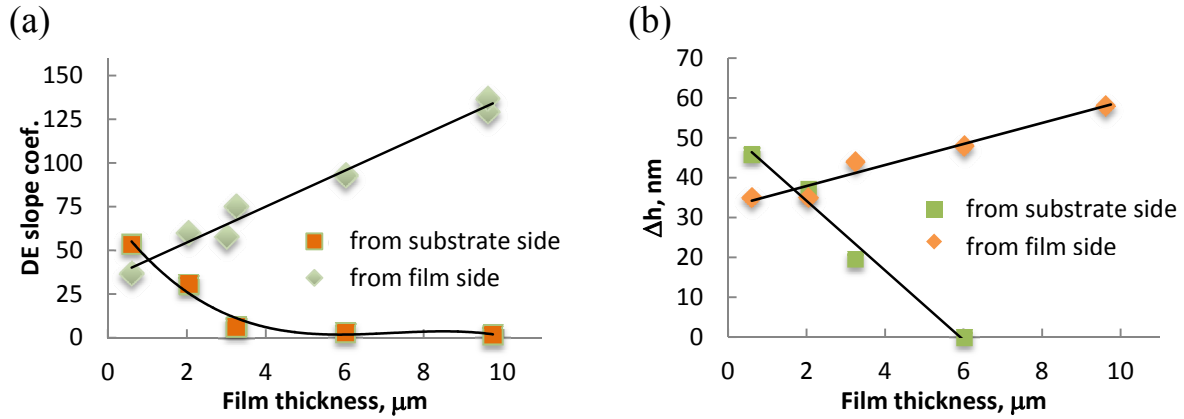


Fig. 3.3. A relative comparison of direct record (a) reflection DE slope coefficient for different As_2S_3 sample thickness of the record from film side and from substrate side, (b) obtained record height comparison in both of these cases *45 and -45 polarization holographic recording was performed by 532nm wavelength ($I_1=I_2=0.25\text{W}/\text{cm}^2$, $\Lambda=1\mu\text{m}$)*

1. Table. Direct recording possibilities in amorphous As_2S_3 thin films *recording was performed by 532nm wavelength ($I_1=I_2=0.25\text{W}/\text{cm}^2$, $\Lambda=1\mu\text{m}$)*

Polarization of the light	Recording efficiency ($\Delta\eta/\Delta t$), $10^{-7}/\text{sek.}$	Relative comparison of direct record
$p + p$	0.35	Good (3)
$s + s$	0.1	Poor (4)
$s + p$	0.04	Ļoti slikti (5)
$45^0 + 45^0$	0.72	Good (2)
$45^0 + -45^0$	44	Very good (1)

3.1.1. Direct record in amorphous thin films

In the previous section we have seen that direct recording process is described by DE curve and thus its precise shape or slope ($\Delta\eta/\Delta t$) describes recording efficiency. We can see from the graphs of figure 3.3a. and 3.3b. that DE slope coefficient curves for different thicknesses of samples describes well obtained surface heights. Comparing the records from the film and the substrate (glass) side, we see that for the holographic recording it is possible to determine active record depth or optimal film thickness, which in this case is approximately 2.5 μm .

Table 1 shows the summary of records with several interfering radiation polarization combinations. After the direct recording evaluation, which is based on the slope coefficient values, we can see that the direct

record is highly dependent on the selected polarization. In order to continue data analysis and determine the divergence of given results, it is necessary to carry out the theoretical interference calculations, which was carried out within this work.

3.1.2. Computer visualizations of plain wave interference

This part describes theoretical intensity distribution of the holographic recording, which is registered by light-sensitive material in which recording takes place. Comparing obtained theoretical two-beam interference distributions (Fig. 3.4.) with previously obtained record efficiency or DE slope coefficient (Table 1), we can conclude that an effective record (eg., -45 and 45 polarizations) does not need a large light intensity gradient. Gradient absence, like in s and p polarization case, also does not guarantee an effective record. To further explore the effect of light on the mass transfer, next part will describe multi-beam interference model and the obtained experimental results.

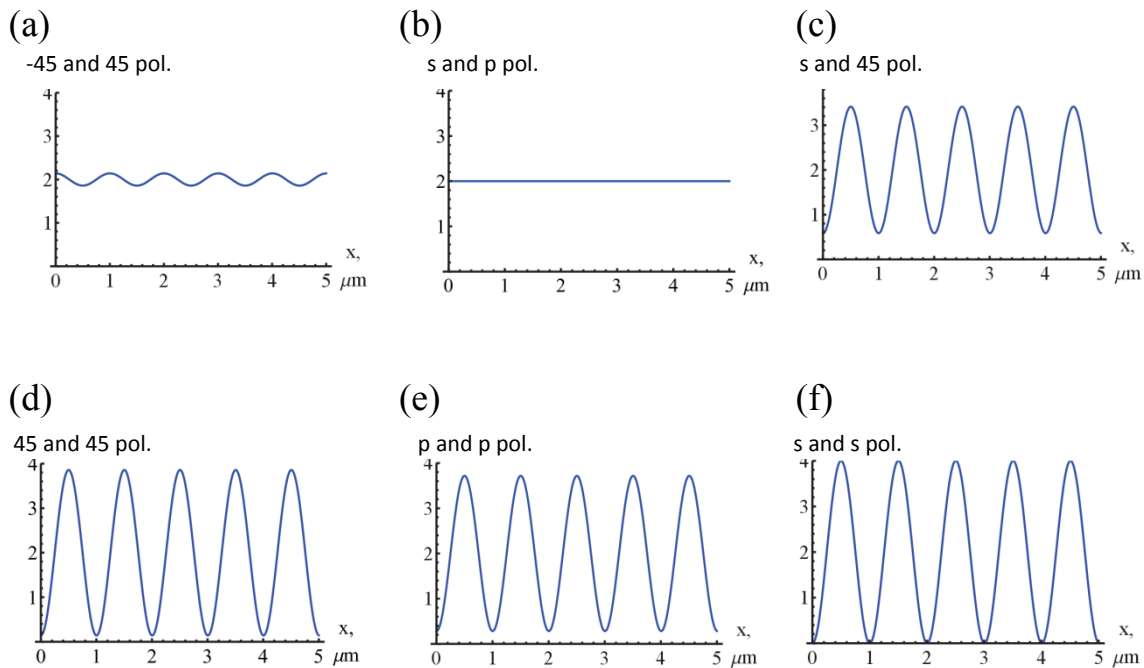


Fig. 3.4. Theoretical intensity distribution for two-beam interference, the angle between light electric field vectors: (a, b) 90 degree, (c) 45 degree and (d, e, f) 0 degree, interference period $\Lambda=1\mu\text{m}$ and $\lambda=532\text{nm}$

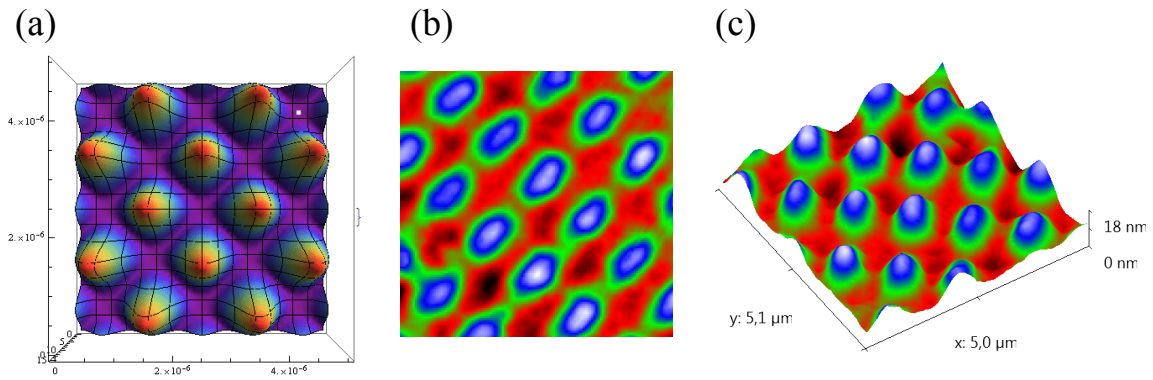


Fig. 3.5. (b, c) AFM pictures of four-beam holographic recording in As-S-Se sample and (a) its comparison with the theoretical light interference intensity distribution

In this case all four beams are with the same polarization direction

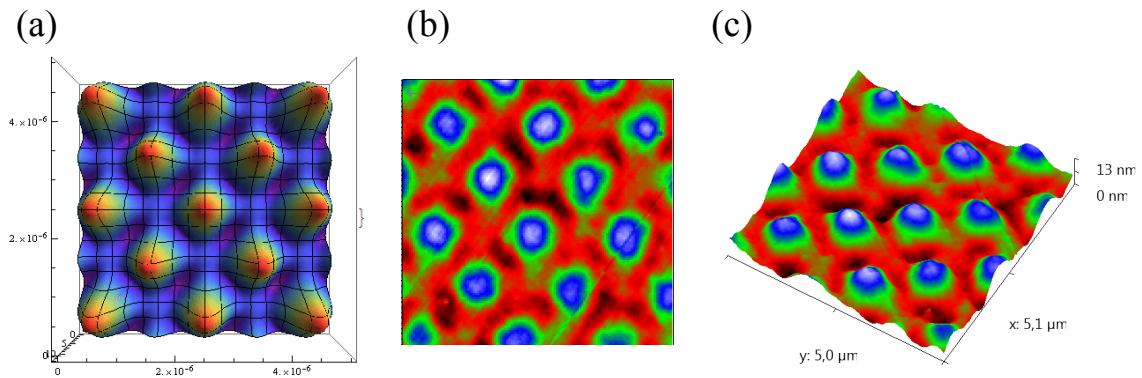


Fig. 3.6. AFM pictures of four-beam holographic recording in As-S-Se sample and (a) its comparison with the theoretical light interference intensity distribution

In this case of two opposite light beams polarization is turned by 45 degrees

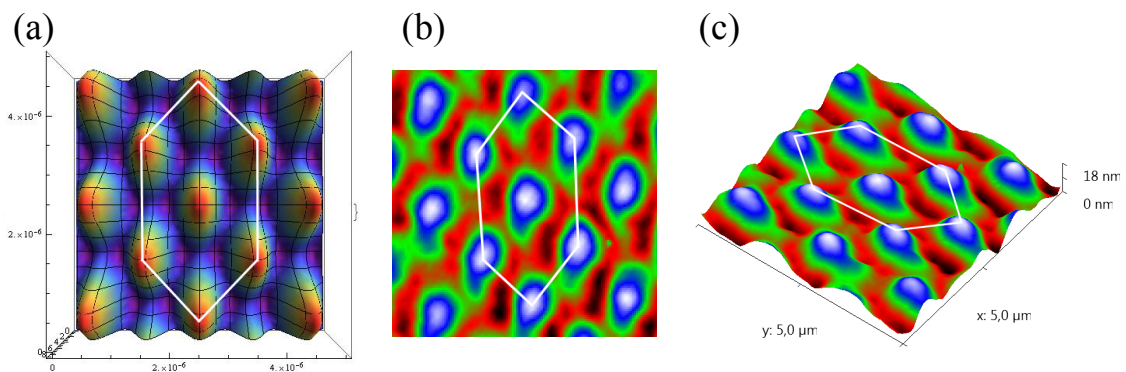


Fig. 3.7. AFM pictures of three-beam holographic recording in As-S-Se sample and (a) its comparison with the theoretical light interference intensity distribution

In this case all three beams are with the same polarization direction

3.1.3. Multi-beam holographic recording experiment comparison with theory

In four-beam holographic setup when all light sources are polarized in the same direction, light interference has highly expressed peaks (16 times more intense than each of the falling light beams) and at minimums light intensity is equal to zero (Fig. 3.5a.). In this holographic recording we can see that the obtained surface relief repeats intensity distribution (Fig. 3.5.). In the case of two opposite light beams polarization is turned by 45 degrees, light intensity gradient is reduced and intensity peaks is not that high, and intensity at minimums also is no longer equal to zero (Fig.3.6a.). In experimental record cases the mass is transferred to the light-intensive areas (Fig.3.6.). An identical situation is observed in three-beam holographic recording when all three sources of light are polarized in one direction (Fig.3.7) - relief repeats theoretical interference intensity distribution.

From the results obtained we can conclude that in this case the mass is transferred towards areas more intensively lit. With multi-beam (three and four-beam) holographic recording equipment it is possible to obtain different types of 3D point intensity distributions and thus also record various 3D structures. Such dot-shaped intensity distributions are attracted not only from the practical point of view, but also from the point of view of sample examination, because it allows to record unique and high-precision structures in one step, which are easy to relate to calculated interference distribution.

3.1.4. Chalcogenide photo-induced softening effect on direct holographic record

This part will describe the efficiency of direct holographic recording and surface relief formation as well as polarization impact anisotropy on recording efficiency. It was found that by using supplemental beam it is possible to improve direct recording efficiency several times. Perhaps, the effect can be associated with the sample softening induced by additional light.

Nd:YAG 532nm laser was used for holographic recording. For supplemental beam semiconductor lasers were selected with a sufficiently large absorption for a given light-sensitive As_2S_3 sample: 448 and 473 nm wavelengths. Fig. 3.8. shows dependence of the recording efficiency

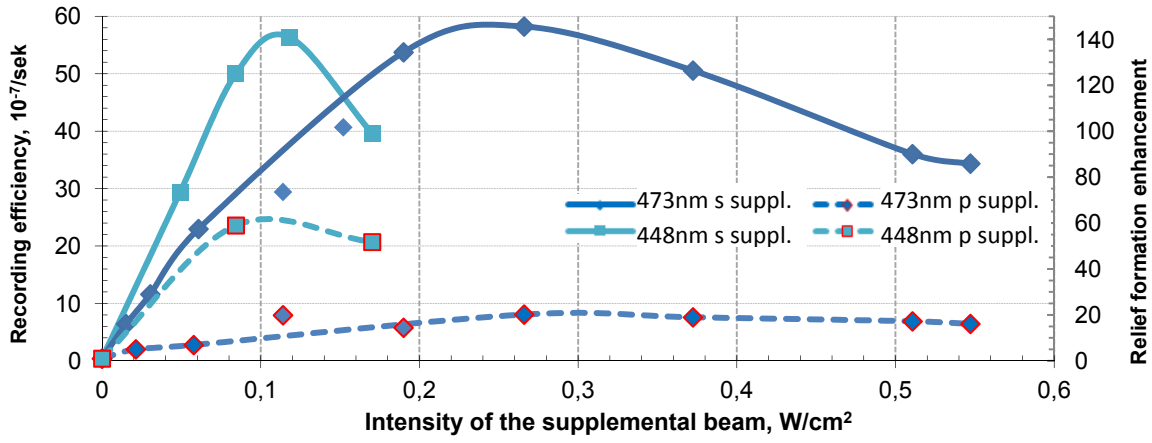


Fig. 3.8. Efficiency of surface relief formation versus intensity of supplemental beam during holographic recording in As_2S_3 thin film
Recording was performed by *p* and *p* polarized 532nm wavelength
($I_1=I_2=0.2\text{W}/\text{cm}^2$, $\Lambda=1\mu\text{m}$)

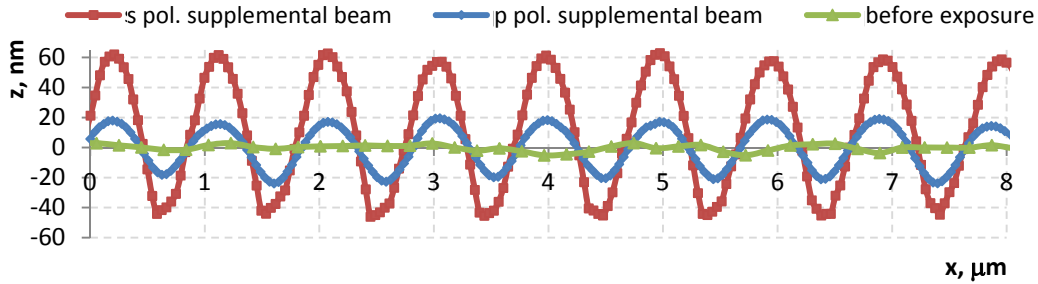


Fig. 3.9. Surface relief profile after recording at 532 nm wavelength p-polarized light ($I_1 = I_2 = 0.2 \text{ W}/\text{cm}^2$) in the case of extra illumination by 473 nm 0.26 W/cm^2 wavelength s-polarized and p-polarized light and its comparison with unexposed spot of the sample (dots: experimental data)
Recording was performed by *p* and *p* polarized 532nm wavelength
($I_1=I_2=0.2\text{W}/\text{cm}^2$, $\Lambda=1\mu\text{m}$)

($\Delta\eta_R/\Delta t$) on its parameters, *i.e.* the efficiency of surface relief formation versus intensity of supplemental beam during holographic recording. Other recording parameters (recording light, its intensity and polarization state (532nm, $0.2\text{W}/\text{cm}^2$ and *p*-polarization)) are constant.

From the Figure we can see that the surface relief formation efficiency changes a lot by increasing intensity of the supplemental beam. All these curves somewhere reaches their maximum, *i.e.* for every wavelength light what is used for extra illumination exist recording conditions for the best performance. By changing supplemental beam wavelength light, maximum performance illumination intensity also varies. As we can see from Fig. 3.8., by changing extra illumination wavelength λ from 448 nm to 473 nm the best performance is reached when $I_{473\text{nm}} = 0.26\text{W}/\text{cm}^2$, which is

different from 448nm case ($I_{448\text{nm}} = 0.11 \text{ W/cm}^2$). This can be explained by the fact that 473 nm is closer to absorption edge of the sample, i.e. for the same effect we need to illuminate it by the light of higher intensity. At light intensities higher than these values, interfering light sources are no longer good enough to form the holographic grating; the sample becomes too fluid, increased light intensity begins to reduce the recording efficiency.

Here (Fig. 3.8., recording by p and p polarized light) we see that the recording efficiency depends not only from the extra illumination wavelength light and its intensity but also from its polarization state. In case of all extra illumination wavelengths (448 nm and 473 nm) the best performance is reached by its s polarization state. Diffraction efficiency and hence the recording efficiency ($\Delta\eta_R/\Delta t$) and the benefit of relief formation (relief recording efficiency without additional lighting standardized to 1) provide only indirect information on the direct holographic recording surface relief amplitude changes during recording. The grid profile measurements were made with atomic force microscopy (AFM). Fig. 3.9. shows the surface morphology AFM profiles induced by holographic recording. The surface of the amorphous chalcogenide As_2S_3 film before holographic recording and the same surface after recording at extra illumination by p and s polarized light are indicated. As it was expected from Fig. 3.8., where the relief formation enhancement for s polarized extra illumination is about 10 times bigger than it is for p polarized, the surface relief is expressed much stronger in the case of s polarized extra illumination. The next part will summarize the results of other types of the recording beam polarization combinations.

3.1.5. Polarization effect on holographic grid record and on supplemental beam

This part looks at what the results are obtained by holographic recording at different polarizations. The record efficiency is compared with the results that were obtained in experiments with different polarizations of 473nm supplemental beam.

Table 2 summarizes the data not only of p and p (denoted as p:p) polarized recording light but also of all other polarization combinations. Here it is important to pay attention to the recording polarization state and the extra illumination polarization state for the maximum performance. As it is shown, the best recording performance without any supplemental beam is reached by opposite circularly (LC:RC) and by +44:-45 (i.e. 45 and 135) degree polarized light. Recorded efficiency of both cases

2. Table. Surface relief formation efficiency versus the polarization combinations of recording and assisting beam
Recording was performed in As_2S_3 films with 532nm wavelength ($I_1=I_2=0.25W/cm^2$, $\Lambda=1\mu m$), 473nm supplemental beam (0 or $0.24W/cm^2$)

Recording setup	Supplemental beam	Recording efficiency ($\Delta\eta/\Delta t$), $10^{-7}/\text{sek.}$	Relief formation enhancement	Relative comparison (w/out suppl. beam)	Relative comparison (with suppl. beam)
$p : p$	s	91	260.0		Very good
	p	13.7	39.1		
	-	0.35	1.0	Good	
$s : s$	s	0.22	2.2		
	p	19	190.0		Good
	-	0.1	1.0	Poor	
$s : p$	s	0.17	4.3		Very poor
	p	0.035	0.9		
	-	0.04	1.0	Very poor	
$45^0 : 45^0$	s	23	31.9		Good
	p	0.2	0.3		
	-	0.72	1.0	Good	
$45^0 : -45^0$	s	102	2.3		Very good
	p	90.4	2.1		
	-	44	1.0		
	45^0	98	2.2	Very good	
$LC : RC$	s	58	0.6		Very good
	p	62	0.7		
	-	90	1.0	Very good	
$LC : LC$ or $RC : RC$	s	57	100.0		Very good
	p	0.25	0.4		
	-	0.57	1.0	Good	

significantly differs from recording of the rest of the polarization combinations. The next section will describe the reasons for these results.

However, when we start to use extra illumination the situation changes. First, we can see that in the case of p:p recording polarization an extra s polarized illumination is needed for the best performance, but in s:s case p polarized illumination, *i.e.* in each of the cases cross-polarized extra illumination is required for equal linear recording polarization states. The situation is different when cross-polarized recording beams are used for holographic recording. For -45 and 45 degree polarized recording beams all polarization states of the extra illumination gives the same results for the best performance, *i.e.* it is not important what kind of light polarization

is been used for extra illumination, we will get the same relief formation enhancement. In the case of circularly-polarized recording light, extra illumination gives an excellent result if both recording beams are polarized in the same direction and the extra illumination light is in spolarization state (enhancement of relief formation is changing from 1 to 100). If both recording beams are oppositely circular polarized, the extra illumination only reduces the efficiency of the surface relief formation.

To explain these results it is necessary to make new theoretical calculations for advanced study of two-beam interference intensity distribution, that is, to study the polarization distribution in case of two-beam interference.

3.1.6. Theoretical polarization distribution for two-beam interference

From the previously observed results (Table 2), we can conclude that there are such recording beam polarization combinations (*e.g.*, -45 and 45) at which direct recording is possible with very high efficiency. Since the calculated intensity distribution in -45:45 case is practically uniform (Fig.3.4a.), there was an idea that the necessary condition for grid recording is the electric field intensity gradient rather than the light intensity gradient. There is very little scientific literature to look at the plane wave interference electric field intensity distributions and it is incomplete (includes only a few cases, lack information or explanation, etc.) and there no result origins shown or explained (mathematical calculations, model, etc.). In order to facilitate the interpretation of experimental results and analysis, this part will describe in theory all the most popular type of the recording beam interference electric field distributions.

In figure 3.10 you can see theoretically calculated two plain wave interference polarization distributions. The black curves represents a total intensity of light interference, which are identical to the results obtained in 3.1.2. section. Two of the intensity distribution components are shown separately: dotted and dashed curves with corresponding masks under them corresponds for the intensity from the polarization directions parallel (p-direction) and perpendicular (s-direction) to the plane of incidence respectively. Note that there is also the third component for intensity distribution that is with radial direction (orthogonal to the s and p direction) but that is comparatively small and is not pointed out. Besides theoretical polarization distribution at the two coherent beams interference versus polarization combinations of the interfering beams are shown in

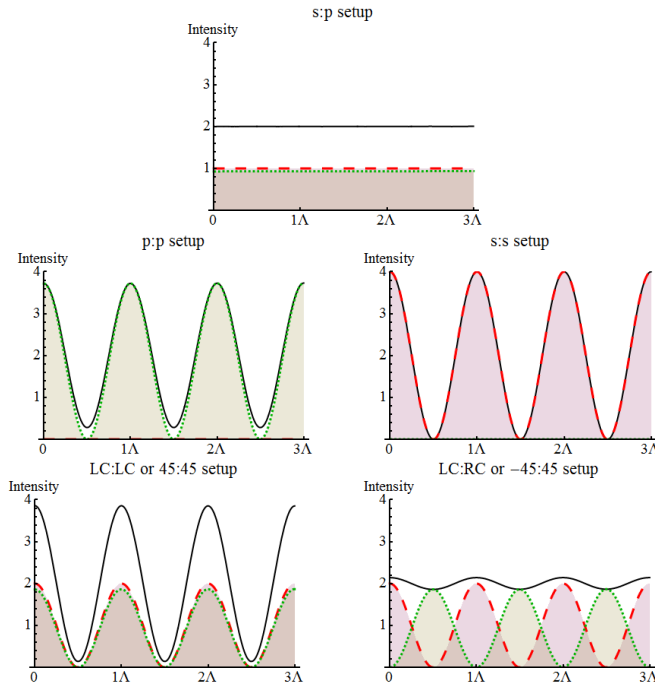


Fig. 3.10. Theoretical light intensity distributions (solid curves) for two coherent beams interference, dashed and dotted curves corresponds to the s and p polarization components respectively. Intensity of the interfered light $I_1=I_2=1$ unit, Λ - period, angle between corresponding \mathbf{k} -vectors $2\alpha=30.86^\circ$, $\Lambda=1\mu\text{m}$, $\lambda=532\text{nm}$

Polarization of the beams		Sum of the electric fields in x-y plane					
first ($I=1$)	second ($I=1$)	$\Delta\phi$:	$-\pi$	$-\pi/2$	0	$+\pi/2$	$+\pi$
		x:	$-\Lambda/2$	$-\Lambda/4$	0	$+\Lambda/4$	$+\Lambda/2$
s \updownarrow	s \updownarrow	n/a	\updownarrow	\updownarrow	\updownarrow	\updownarrow	n/a
		I:	0.00	2.00	4.00	2.00	0.00
p \leftrightarrow	p \leftrightarrow	•	\leftrightarrow	\leftrightarrow	\leftrightarrow	\leftrightarrow	•
		I:	0.28	2.00	3.72	2.00	0.28
s \updownarrow	p \leftrightarrow	\swarrow	\circ	\swarrow	\circ	\swarrow	\circ
		I:	2.00	2.00	2.00	2.00	2.00
+45 \swarrow	-45 \searrow	\leftrightarrow	\circ	\updownarrow	\circ	\leftrightarrow	\circ
		I:	1.86	2.00	2.14	2.00	1.86
-45 \swarrow	-45 \searrow	•	\swarrow	\swarrow	\swarrow	\swarrow	•
		I:	0.14	2.00	3.84	2.00	0.14
RC \circ	RC \circ	•	\circ	\circ	\circ	\circ	•
		I:	0.14	2.00	3.86	2.00	0.14
RC \circ	LC \circ	\leftrightarrow	\swarrow	\updownarrow	\swarrow	\leftrightarrow	\circ
		I:	1.86	2.00	2.14	2.00	1.86

Fig. 3.11. Theoretical polarization distribution at the two coherent beams interference versus polarization combinations of the interfering beams. Intensity of the interfered light $I_1=I_2=1$ unit, Λ - period, angle between corresponding \mathbf{k} -vectors $2\alpha=30.86^\circ$, $\Lambda=1\mu\text{m}$, $\lambda=532\text{nm}$

Fig. 3.11. There can see not only a absolute values of the intensities for different phase shifts $\Delta\phi$ ($-\pi$; $-\pi/2$; 0; $\pi/2$ and π) but also corresponding polarization distribution for all combinations of the interfered light polarizations.

Now if compare previously arranged polarization combinations by impact on direct SRG formation quality (Table 2) with theoretically calculated polarization components of the intensity distribution at Fig.3.10., it is clearly seen that for best direct recording possibilities (45° :- 45° or LC:RC setup) instead of high intensity gradient needs electric field gradients— s and p components with are a half-cycle out of phase. That is most likely to be responsible for the high recording efficiency- s and p polarized light gradients with a half-cycle out of phase helps each other to form a SRG, *i.e.*, on both of the periodic gradients the matter interacts differently. In case of just one s or p component electric field gradient (s:s or p:p setup) or when both the components are in phase ($45:45$ or LC:LC

setup) or without gradient (s:p setup) it is possible to get just poor kind of SRG structures.

Experiments show that for some polarization combinations of the writing beams are possible to dramatically increase recording efficiency by supplemental illumination during direct SRG formation process (Table 2). Supplemental beam does not interfere with the light from writing beams and just extra soften the sample. The idea and explanation of this process is as follows: by using extra illumination to make intensity distribution more alike it is for 45:-45 or LC:RC setup with a half-cycle out of phase for s and p intensity components, therefore to make recording efficiency as good as it is for 45:-45 and LC:RC setup. And as expected, extra illumination with polarization orthogonal to the polarization of the interfered light (Table 2) gives best SRG formation enhancing effects. For example, p:p polarization setup previously arranged as a *poor* one combination for formation of the SRG, now with extra s polarized light illumination is as best as it is for 45:-45 or LC:RC polarization setup with or without extra illumination. In fact, extra illumination for 45:-45 or LC:RC setup just decrease SRG formation efficiency.

In other words, the most efficient record will be in the case where the periodic interference s and p components are in opposite phases and they *help* each other at the same time to form a hill and a ditch. Each of the components is responsible for one of these processes. Next parts will be dedicated to detailed research of this process and explanation of ongoing events during recording.

3.1.7. Mass transfer direction during the holographic recording based on the foto-induced birefringence

If we consider various combinations of polarization in the case of holographic recording it has been determined that the highest possible modulation of direct SRG recording can be achieved only in two cases – using -45:45 degree and circular:anti-circular (RC:LC) polarization. Both of these combinations stand out in the theoretical interference pattern calculations (shown in Figure 3.10.). The contrast in these cases is very close to zero – almost uniform intensity distribution, but the electric field intensity distribution contains s and p components which are in opposite phases and the contrast for each component is 1 (shown in Figure 3.10. as shaded parts). Since in monolayers of amorphous chalcogenides (and other certain photo-resist materials) this direct-recording process is reversible,

there is only one possibility for the lateral mass transfer and that will be discussed in this section.

During holographic recording the mass moves parallel to the intensity gradient and in an opposite direction with respect to the polarization of the electric field intensity gradient. It can be verified experimentally with this holographic recording setup by changing polarization of the probe beam from p- to s-polarization and/or vice versa for the same experiment. The dotted and dashed curves in Figure 3.12a. and 3.12b. show the dependence of transmission DE on p- and s- probe beam polarization state, respectively. At the start-up phase where the transmission drops, the formation of bulk phase gratings is monitored: the transmission curve clearly saturates and the peak in the diffraction efficiency of p-polarization probe beam appears (shown in Figure 3.12c.). For the s-polarized probe beam no maximum in DE was observed at this point, which can be explained by the photo-induced birefringence Δn .

In covalent chalcogenide glasses the birefringence is negative, *i.e.*, $\Delta n = n_{\parallel} - n_{\perp} < 0$ [65], where n_{\parallel} and n_{\perp} are the refractive indices parallel and perpendicular to the electric field of excitation light, respectively. Therefore, before holographic recording refractive index for the As_2S_3 film is isotropic with respect to the polarization of the light. At the first recording seconds periodic refractive index starts to form a bulk phase grating. (see simplified model in Figure 3.12d.). At the refractive index grating drawing the polarization components of the interference pattern are randomly attached (like in -45: 45 model in Fig. 3.10).

By taking into account that $\Delta n < 0$, for the s-polarized (3-1) and p-polarized (3-2) probe beam:

$$n_1 \cdot h_0 > n_2 \cdot h_0 \quad 3-1$$

$$n_1 \cdot h_0 < n_2 \cdot h_0 \quad 3-2$$

where h_0 thickness of the As_2S_3 film. This difference between $n_1 h_0$ and $n_2 h_0$ grows and DE increases for both of them until surface-relief formation takes place. Then for the s-polarized (3-3) and p-polarized (3-4) probe beam:

$$n_1 \cdot h_1' > n_2 \cdot h_2' \quad 3-3$$

$$n_1 \cdot h_1' < n_2 \cdot h_2' \quad 3-4$$

where h_i' thickness of the As_2S_3 film during SRG formation. Subsequently h_1' increases and h_2' decreases or vice versa. As mentioned above, at the start-up phase for the p-polarized probe beam a maximum in DE appears whereas for the s-polarized beam- not. It can be only explained by the fact that h_1' increases and h_2' decreases during the direct holographic recording. Therefore for the s-polarized probe beam where n_1, h_1' are

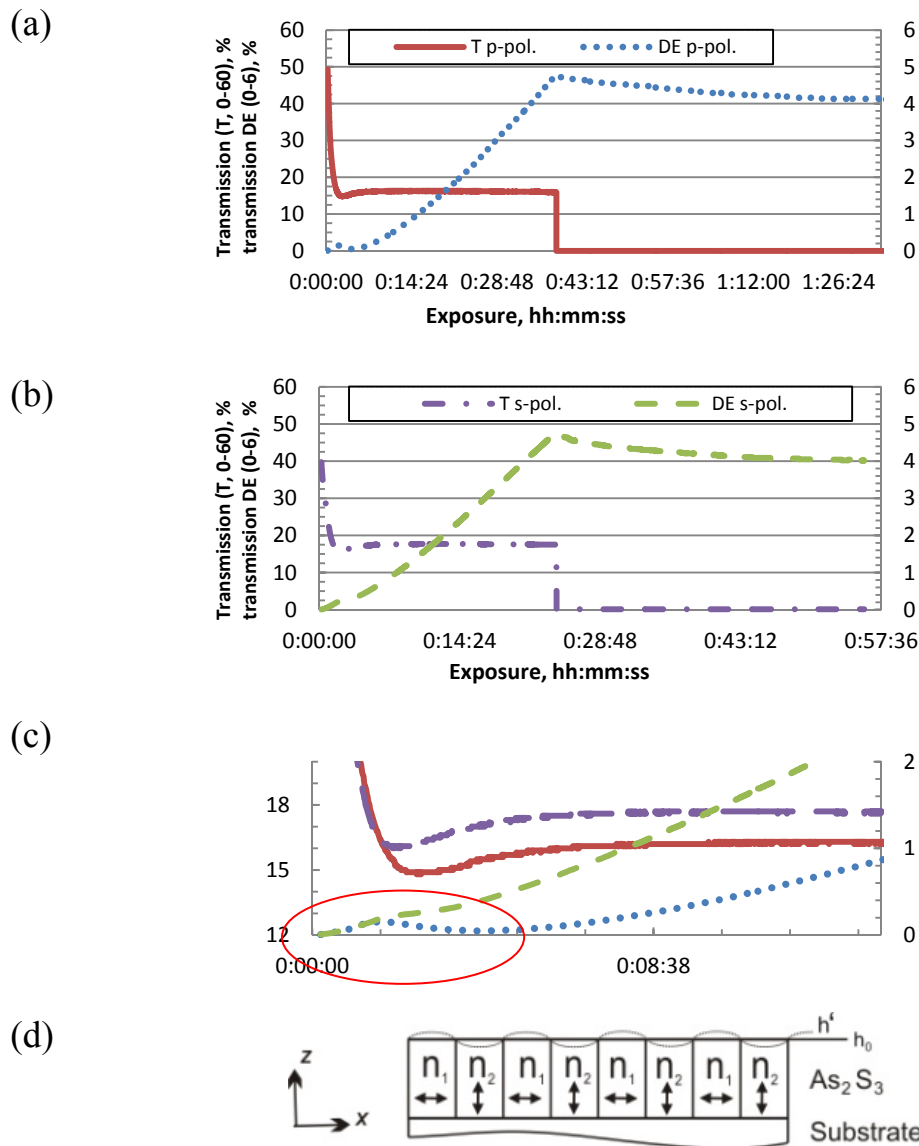


Fig. 3.12. (a) and (b) Transmission of the writing beam (solid and dashed-dotted curves) and diffraction efficiency from the probe beam (dotted and dashed curves) of a two holographic recording experiments shows dependency from the probe beam polarization state, (c) its start-up phase and (b) simplified SRG formation model

Recording was made in As_2S_3 sample by -45 and 45 degree polarization

increasing and n_2 , h_2' are decreasing, the DE curve rises continuously. Other sequence of events is for the p-polarized probe beam where n_2 , h_1' are increasing and n_1 , h_2' are decreasing during recording. At the beginning formation of bulk phase gratings occurs, which causes the growth of DE. Afterwards newly formed surface-relief starts to erase DE thus a maximum appears. Following is a steady increase of DE because $\Delta h_i'$ takes over Δn_i , which is true for both polarizations.

To investigate the behavior of newly produced surface-relief gratings, relaxation of the DE for the p- and s-polarized probe beam was monitored:

when DE reached $\sim 4.6\%$ (dotted and dashed curves in Figure 3.12.) the writing laser was switched off and after that the DE of both polarizations relaxed to $\sim 4\%$. Therefore it is possible to obtain large area and high quality gratings which are very stable at a room temperature.

3.2. Direct recording and its research after the sample irradiation through narrow slit

In order to experimentally verify mass transfer direction and intensity of the electric field gradient interconnections in previous sections, a new record scheme was created (see scheme in Fig. 2.1b). Main component of the scheme is approximately $10\mu\text{m}$ wide slit, which ideally allows irradiating the sample with a rectangular light intensity distribution. When realizing such uniform intensity distribution record, it is possible to study the surface relief formation in a completely controlled environment, where the polarization can be assumed to be the same and constant in both time and space. Since this recording beam falls perpendicular to the sample surface, the polarization is defined according to the slit direction: in case of parallel polarization (s direction) it is possible to simulate one period record of holographic recording in s+s case. In perpendicular polarization case (p direction) one period of p+p holographic record is simulated.

3.2.1. Mass transfer direction

Previously viewed holographic recording only indirectly explains the mass transfer processes during the record. Using a narrow slit record scheme, it is possible to determine by just measuring obtained topography on AFM. The first obtained recordings independently from the polarization were insignificant (few nm in height) and could be attributed to photo-induced expansion effect [66]. As previous experiments with direct holographic recordings showed that relief forming efficiency can be significantly improved by additional incoherent assisting beam, the same approach was utilized for further experiments. The symbol a/b denotes the possible combinations of polarization, a – for the recording beam and b – for the assisting beam. As we will see below, such recording setup gives a significant improvement of the record.

Realizing the first s and p polarization records with orthogonally polarized supplemental beam, we can see that there may be two different mass transfer directions (Fig. 3.13). So, s polarized light intensity gradient, stimulated by p polarized supplemental beam (s/p record), creates around

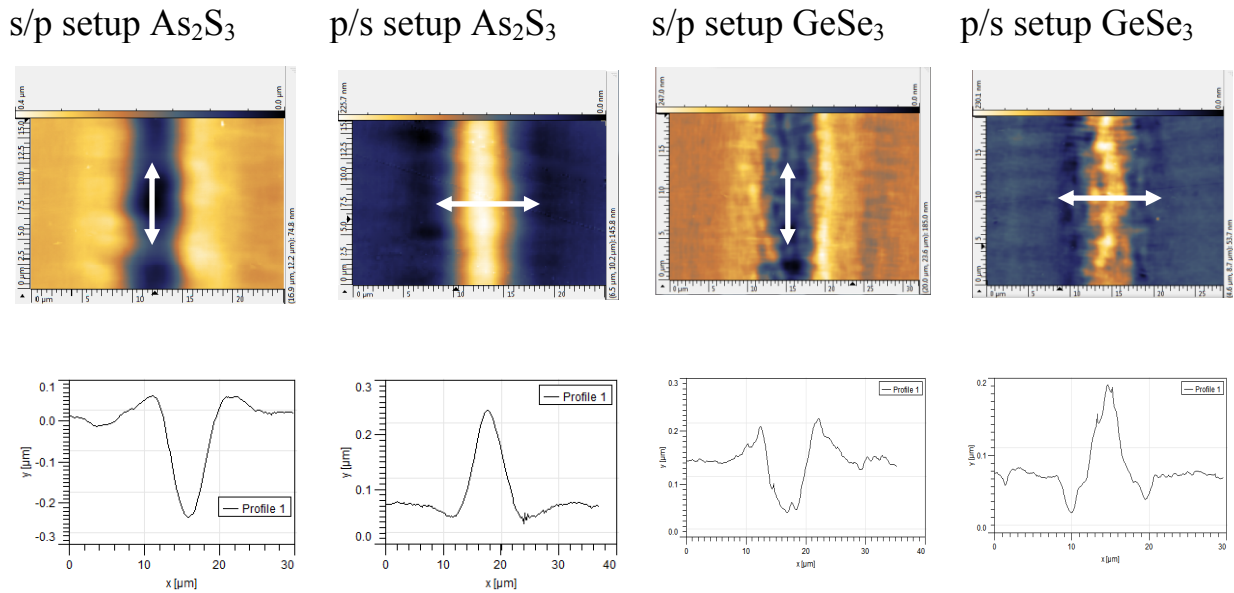


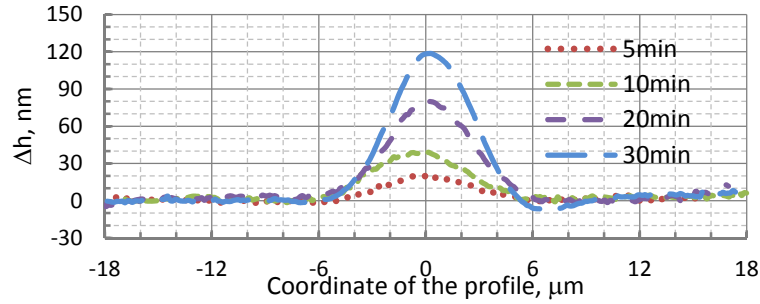
Fig. 3.13. S polarized (s/p setup) and p polarized (p/s setup) light intensity gradient's effect on mass transfer direction in As_2S_3 and GeSe_3 films
Direction of the writing light electric field illustrated with arrows

10 μm wide ditch. Accordingly, the p-polarized light intensity gradient, stimulated by s polarized supplemental beam (p/s recording), creates a hill with the same width. We can conclude that the s polarization light intensity gradient pushes off mass particles, but p polarization light intensity gradient is pulling the mass particles. Conclusions of results obtained here fully correspond to conclusions in 3.1.7 section.

3.2.2. Development of the record in optical slit experiment in time

As mentioned above, in the case of different polarization of the writing beams the direction of mass transfer is opposite. For the s polarization (s/p setup: polarization of the writing beam is parallel to the slit) the mass is transported away from the illuminated area thus forming a groove, but for the p polarization (p/s setup) this process is inverted – the mass is transported into the illuminated area, forming a ridge. Note that the assisting beams were polarized orthogonally to the writing. Formation of relief, depending on the different recording parameters (mainly from the recording time and recording beam intensity) will be view in detail in this section. It is clearly seen that for the both recording setups (p/s and s/p) the mass transfer starts from the middle of 10 μm optical slit used in these experiments (Fig. 3.14.). For the short time exposure (in this case up to 10 min) A- or V-shaped profiles appear. If the recording time exceeds 10 minutes an active mass squeezing takes place and the profiles are changing

(a) recording polarization is parallel to the gradient



(b) recording polarization is orthogonal to the gradient

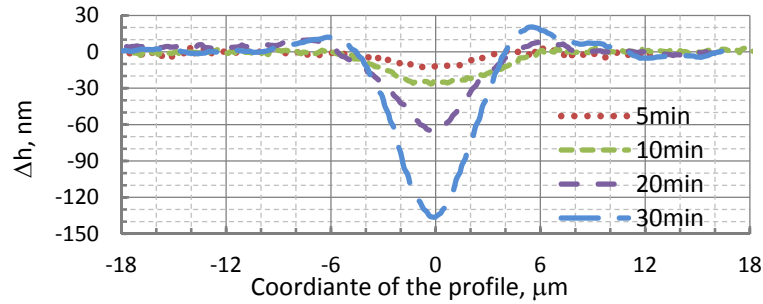


Fig. 3.14. The time evolution of SRG profiles extracted from the AFM measurements, recording performed on the As_2S_3 sample with a: (a) p/s and (b) s/p setup. The energy densities for the writing and assisting beam were $4.24\text{W}/\text{cm}^2$ and $0.37\text{W}/\text{cm}^2$ respectively, corresponding exposure lengths: 5, 10, 20 and 30 minutes

to W- or M- shaped. Such type of recording progress show that all of the volume participates in relief formation process and not just the top layer.

3.2.3. Overview of the optical slit experiments

By inserting $\frac{1}{2}$ and/or $\frac{1}{4}$ wave plates into the scheme, it is possible to vary the recording and supplemental beam polarization and obtained record reliefs measure with *Veeco CPII* AFM. Such overview of experimental results will be described in this section.

In Fig. 3.15. the summary of obtained results has been presented as table. Certain cells are carrying a value *w/out* – this means that with such polarization configuration the obtained relief is insignificant (few nm) and basically represents smooth surface. Without supplemental beam, insignificant record was observed at all recording beam polarizations (not marked in the figure). The remaining cells which do carry values different from zero are represented by AFM images and profile height distributions. Looking at the record polarization combinations, of which the relief record is formed, we can already draw more conclusions about polarized light intensity gradient effect on the sample.

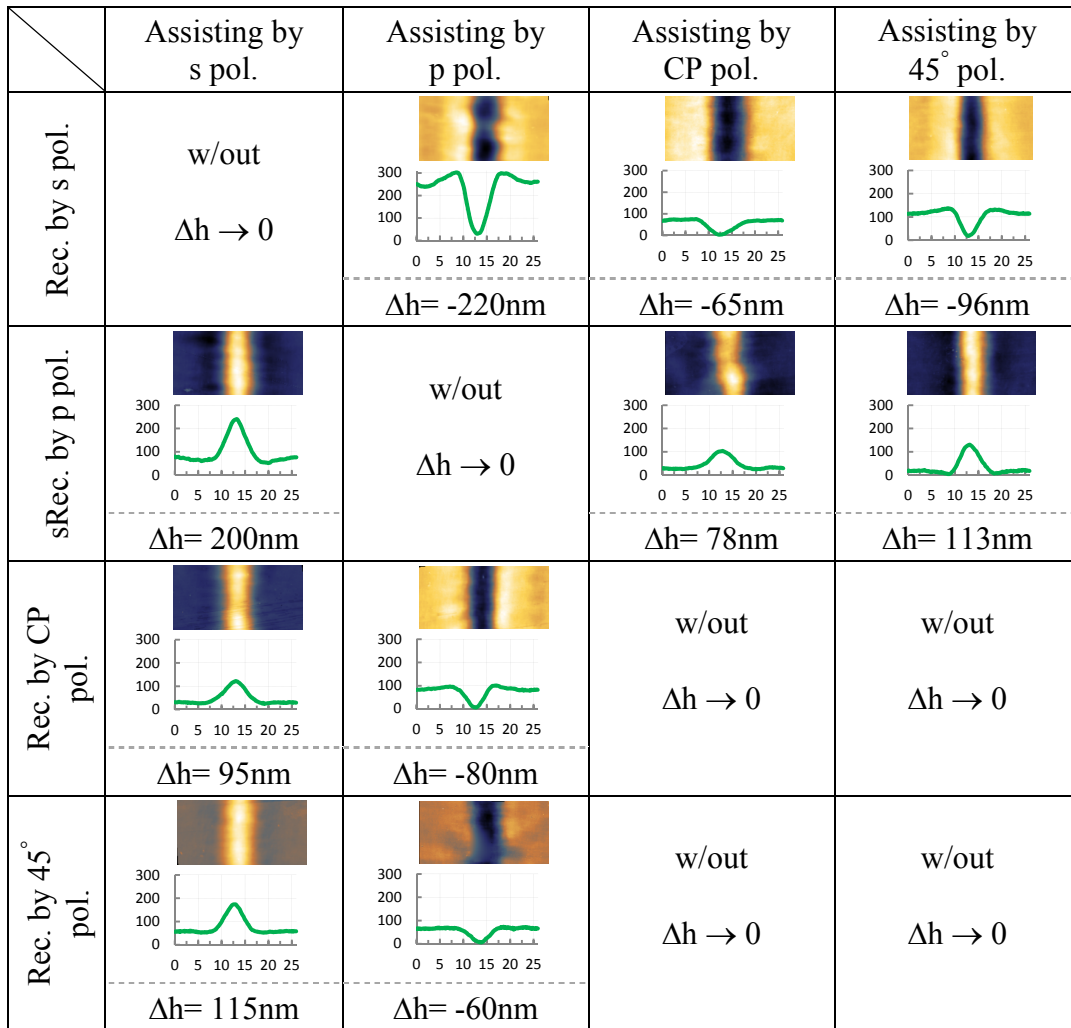


Fig. 3.15. The correlation between polarization and light-induced mass transfer processes in 2.1 μm thin layer of As_2S_3 sample for different polarization combinations of the writing and assisting beams (1000 mW/cm^2 and 1500 mW/cm^2 for 1 h respectively) in optical slit experiments. The inset contains the 2D $26 \times 13 \mu\text{m}$ AFM topography pictures and its profiles in the $25 \mu\text{m} \times 300\text{nm}$ frame

If the polarization of recording beam coincides with the direction of optical slit (defined as s-polarization), then independently from the polarization of the assisting beam (1st row in Fig. 3.15.: CP- circular, p-perpendicular to the slit or 45 degree) a mass transfer away from the recording region can be observed – formation of a groove. The efficiency of recording or the depth of groove changes from the best case, when the polarization of assisting beam is perpendicular to that of the recording beam, then follows the 45 degree and finally CP polarization. The same applies when the polarization of recording beam is perpendicular to the slit (2nd row in Fig.3.15.), only in this case mass transfer is directed towards recording region – formation of a ridge. The polarization of recording

beam is not the only factor, which determines the direction of mass transfer. Independently from the polarization of recording beam, consistent formation of a ridge, when the assisting illumination is s-polarized (1st column in Fig.3.15.) or formation of a groove, when assisting illumination has p-polarization (2nd column in Fig.3.15.), can be observed.

All recording combinations are symmetrically aligned in respect to the main diagonal of the table in Fig. 3.15. This observation means that the polarization of both – recording as well as supplemental beam play a significant role in the process of mass transfer. Without supplemental beam, mass transfer was not observed at all recording beam polarizations. As can be seen the most effective mass transfer occurs when s and p polarization combinations between recording and supplemental beams are implemented and in this case the height was around 200 nm. It is possible to obtain even better results by adjusting intensity of the recording and assisting beams as well as adjusting exposure time.

CONCLUSIONS

Within the doctoral work, all the set tasks were performed, including the deliberate direct recording efficiency depending on parameters (intensity and polarization) and recording conditions, studied both intensity and polarization distribution theoretical model for different beam interference cases. Using a unique and relatively simple equipment, a research was made in direct recording possibilities and mass shift directions with a rectangular light intensity distribution at various light intensities polarizations and record durations.

As it has already been mentioned, during holographic recording, illuminating with incoherent supplemental beam, it is possible to increase the effectiveness grating recording - in some cases even more than a hundred times. Acquired gratings are high quality and practically cannot be acquired with etching or lithography, nor any other method. By supplementary lighting the sample, it is possible to greatly reduce a record time, and also to improve the quality and conducting technologies. The acquired holographic grating is stable at room temperature and, together with the real-time surface relief record amplitude control, the obtained knowledge and technology can find a practical use in optics (holography, lithography, anti-reflection coatings, solar batteries etc.) and electronics (micro and nano matrix design), as well as in nanotechnologies (top-down approach) and many other sectors.

THESIS

1. **Effective direct holographic recording** in amorphous chalcogenide thin films **is possible in cases when recording beams are with -45 and 45 degrees polarization or with opposite circular polarization;**
2. **It is possible to improve the effectiveness of direct holographic recording many times, by using incoherent supplemental beam during the recording;**
3. The drift of mass particles is seen due to light electric field intensity gradient, and **mass drift direction depends on this gradient and the mutual location of electric field direction;**
4. **For a direct holographic recording, it is possible to determine the active recording's depth** or optimal film thickness by comparing recordings from the film side and from the base (glass) side.
5. The use of narrow gap or **rectangular light intensity gradient** in the direct recording, **simulates holographic equipment's a single period recording** in light sensitive material.

REFERENCES

- [1] Y. Kaganovskii, M. L. Trunov, C. Cserhati, P. M. Lytvyn, D. L. Beke, and S. Kökényesi, "Electron-beam induced variation of surface profile in amorphous As₂₀Se₈₀ films" *J. Appl. Phys.*, vol. 115 (18), p. 183512, 2014.
- [2] A. Kikineshi, V. Palyok, I. A. Szabó, M. Shipljak, I. Ivan, and D. L. Beke, "Surface deformations and amplitude-phase recording in chalcogenide nanolayered structures," *J. Non-Cryst. Solids*, vol. 326&327, pp. 484-488, 2003.
- [3] R. P. Wang, *Amorphous Chalcogenides: Advances and Applications*: Pan Stanford Publishing, 2014.
- [4] A. Kikineshi, V. Palyok, M. Shiplyak, I. A. Szabo, and D. L. Beke, "Photo- induced surface deformation during hologram recording in a-Se films," *J. of Optoelectronics and Adv. Materials* vol. 2 (1), pp. 95-98, 2000.
- [5] S. Kokenyesi, I. Iván, V. Takátsa, J. Pálkása, S. Birib, and I. A. Szabo, "Formation of surface structures on amorphous chalcogenide films," *J. Non-Cryst. Solids*, vol. 353 (13-15), pp. 1470–1473, 2007.
- [6] V. Palyok, I. A. Szabó, D. L. Beke, and A. Kikineshi, "Surface grating formation and erasing on a-Se films," *Appl Phys A*, vol. 74 (5), pp. 683-687, 2002.
- [7] U. Gertners and J. Teteris, "Photo-induced Mass Transfer in Chalcogenides," *IOP Conf. Series: Materials Science and Engineering*, vol. 23, p. 012007, 2011.
- [8] K. E. Asatryan, T. Galstian, and R. Vallée, "Optical Polarization Driven Giant Relief Modulation in Amorphous Chalcogenide Glasses," *Phys Rev Lett*, vol. 94 (8), p. 087401, 2005.
- [9] M. Reinfelde, R. Grants, and J. Teteris, "Photoinduced mass transport in amorphous As-S-Se films," *P hys. Status Solidi C*, vol. 9 (12), pp. 2586–2589, 2012.
- [10] S. K. Tripathy, N. K. Viswanathan, S. Balasubramanian, and J. Kumar, "Holographic fabrication of polarization selective diffractive optical elements on azopolymer film," *Polym Adv Technol* vol. 11 (8 12), pp. 570-574, 2000.
- [11] P. Rochon, A. Natansohn, C. L. Callendar, and L. Robitaille, "Guided mode resonance filters using polymer films," *Appl Phys Lett*, vol. 71 (8), pp. 1008-1010, 1997.
- [12] R. J. Stockermans and P. L. Rochon, "Narrow band resonant grating waveguide filters constructed with azobenzene polymers," *Appl Opt* vol. 38 (17), pp. 3714-3719, 1999.
- [13] J. Paterson, A. Natansohn, P. Rochon, C. L. Callendar, and L. Robitaille, "Optically inscribed surface relief diffraction gratings on azobenzene containing polymers for coupling light into slab waveguides," *Appl Phys Lett* vol. 69 (22), pp. 3318-3320, 1996.
- [14] T. Nagata, T. Matsui, M. Ozaki, K. Yoshino, and F. Kajzar, "Novel optical properties of conducting polymer photochromic polymer systems," *Synth Met* vol. 119 (1 3), pp. 607-608, 2001.
- [15] V. Dumarcher, L. Rocha, C. Denis, C. Fiorini, J. M. Nunzi, F. Sobel, *et al.*, "Polymer thin film distributed feedback tunable lasers," *J Opt A: Pure Appl Opt* vol. 2 (4), pp. 279-283, 2000.
- [16] L. Rocha, V. Dumarcher, C. Denis, P. Raimond, C. Fiorini, and J. M. Nunzi, "Laser emission in periodically modulated polymer films," *J Appl Phys* vol. 89 (5), pp. 3067-3069, 2001.
- [17] C. Egami, Y. Kawata, Y. Aoshima, S. Alasfar, O. Sugihara, H. Fujimura, *et al.*, "Two stage optical data storage in azo polymers," *Jpn J Appl Phys* vol. 39 (3B), pp. 1558-1561, 2000.
- [18] P. S. Ramanujam, M. Pedersen, and S. Hvilsted, "Instant holography," *Appl Phys Lett* vol. 74 (21), pp. 3227-3229, 1999
- [19] R. Zallen, *The Physics of Amorphous Solids*: Wiley-VCH, 1998.

- [20] A. Csik, M. Malyovanika, J. Dorogovicsa, A. Kikineshia, D. L. Beke, I. A. Szabo, *et al.*, "Photo-stimulated structural transformations and optical recording in amorphous semiconductor multilayers," *J Optoelectronics and Adv. Materials*, vol. 3 (1), pp. 33-36 2001.
- [21] M. Fischer, T. Galstian, R. Vallée, and A. Saliminia, "Surface and volume contributions to total diffractive efficiency in As₂S₃ thin film glasses " *Synthetic Metals*, vol. 127 (1-3), pp. 303-306, 2002.
- [22] T. V. Galstyan, J. F. Viens, A. Villeneuve, K. Richardson, and M. A. Duguay, "Photoinduced Self-Developing Relief Gratings in Thin Film Chalcogenide As₂S₃ Glasses," *Lightwave Technology*, vol. 15 (98), pp. 1343 - 1347 1997.
- [23] Y. Hayasaki and D. Kawamura, "High-density bump formation on a glass surface using femtosecond laser processing in water," *Appl. Phys. A*, vol. 87 (4), pp. 691-695, 2007.
- [24] A. Kikineshi, "Light-stimulated structural transformations and optical recording in amorphous nano-lauered structures," *J Optoelectronics and Adv. Materials*, vol. 3 (2), pp. 377-0382, 2001.
- [25] V. Palyok and M. Malyovanik, "Photoinduced extension and optical recording in a-Se/As₂S₃ multilayers," *J Optoelectronics and Adv. Materials*, vol. 1 (3), pp. 77-80, 1999.
- [26] J. U. Park, W. S. Kima, and B. S. Bae, "Photoinduced low refractive index in a photosensitive organic-inorganic hybrid material," *J. Mater. Chem.*, vol. 13, pp. 738-741, 2003.
- [27] E. Spanakis, E. Stratakis, and P. Tzanetakis, "Metastable photoexpansion of hydrogenated amorphous silicon produced by exposure to short laser pulses," *J. Non-Cryst. Solids*, vol. 352 (5), pp. 429-433, 2006.
- [28] M. L. Trunov, "Photoplastic effect in non-crystalline materials: a nanoindentation study," *J Physics D: Appl Physics*, vol. 41, p. 074011 2008.
- [29] H. Ukita, H. Uemi, and A. Hirata, "Near Field Observation of a refractive Index Grating and a Topographical Grating by an Optically-Trapped Gold Particle," *Opt. Rev.*, vol. 11 (6), pp. 1-5, 2004.
- [30] C. Vass, K. Osvay, and B. Hopp, "Fabrication of 150 nm period grating in fused silica by two-beam interferometric laser induced backside wet etching method," *Opt Express*, vol. 14 (18), pp. 8354-8359, 2006.
- [31] F. S. D. Vicente, M. S. Li, and Y. Messaddeq, "Holographic recording in [Sb(Po-3)(3)](n)-Sb₂O₃ glassy films by photoinduced volume and refraction index changes," *J. Non-Cryst. Solids*, vol. 348, pp. 245-249, 2004.
- [32] R. Bachelot, F. H'Dhili, D. Barchiesi, G. Lerondel, R. Fikri, P. Royer, *et al.*, "Apertureless near-field optical microscopy: A study of the local tip field enhancement using photosensitive azobenzene-containing films," *J. Appl. Phys.*, vol. 94, pp. 2060-2072 2003.
- [33] S. Bian, L. Li, J. Kumar, D. Y. Kim, J. Williams, and S. K. Tripathy, "Single laser beam-induced surface deformation on azobenzene polymer films " *Appl. Phys. Lett.*, vol. 73, p. 1817 1998.
- [34] C. Cojocariu and P. Rochon, "Light-induced motions in azobenzene-containing polymers," *Pure Appl. Chem.*, vol. 76 (7-8), pp. 1479-1497, 2004.
- [35] C. Fiorini, N. Prudhomm, G. d. Veyrac, I. Maurin, P. Raimond, and J. M. Nunzi, "Molecular migration mechanism for laser induced surface relief grating formation," *Synthetic Metals*, vol. 115 (1-3), pp. 121-125, 2000.
- [36] Y. He, J. Yin, P. Che, and X. Wang, "Epoxy-based polymers containing methyl-substituted azobenzene chromophores and photoinduced surface relief gratings," *European Polymer Journal*, vol. 42 (2), pp. 292-301, 2005.

- [37] H. Ishitobi, M. Tanabe, Z. Sekkat, and S. Kawata, "Nanomovement of azo polymers induced by metal tip enhanced near-field irradiation," *Appl. Phys. Lett.*, vol. 91, p. 091911 2007.
- [38] P. Karageorgiev, D. Neher, B. Schulz, B. Stiller, U. Pietsch, M. Giersig, *et al.*, "From anisotropic photo-fluidity towards nanomanipulation in the optical near-field," *Nat. Mater.*, vol. 4, pp. 699-703 2005.
- [39] D. Y. Kim, S. K. Tripathy, L. Li, and J. Kumar, "Laser-induced holographic surface relief gratings on nonlinear optical polymer films," *Appl. Phys. Lett.*, vol. 66, pp. 1166-1168, 1995.
- [40] N. Koyayashi, C. Egami, and Y. Kawata, "Optical Storage Media with Dye-Doped Minute Spheres on Polymer Films," *Opt. Rev.*, vol. 10, pp. 262-266 2003.
- [41] F. L. Labarthe, J. L. Bruneel, T. Buffeteau, and C. Sourisseau, "Chromophore Orientations upon Irradiation in Gratings Inscribed on Azo-Dye Polymer Films: A Combined AFM and Confocal Raman Microscopic Study," *J. Phys. Chem. B*, vol. 108, pp. 6949-6960 2004.
- [42] K. Munakata, K. Harada, M. Itoh, S. Umegaki, and T. Yatagai, "A new holographic recording material and its diffraction efficiency increase effect the use of photoinduced surface deformation in azo-polymer film," *Opt. Commun.*, vol. 191, pp. 15-19 2001.
- [43] L. L. Nedelchev, A. S. Matharu, S. Hvilsted, and P. S. Ramanujam, "Photoinduced anisotropy in a family of amorphous azobenzene polyesters for optical storage," *Appl. Opt.*, vol. 42, pp. 5918-5927 2003.
- [44] P. Rochon, E. Batalla, and A. Natansohn, "Optically induced surface gratings on azoaromatic polymer films," *Appl. Phys. Lett.*, vol. 66, pp. 136-138 1995.
- [45] C. J. Barrett, P. L. Rochon, and A. L. Natansohn, "Model of laser driven mass transport in thin films of dye functionalized polymers," *J Chem Phys* vol. 109 (4), pp. 1505-1516, 1998.
- [46] T. Fukuda, K. Sumaru, T. Yamanaka, and H. Matsuda, "Photo induced formation of the surface relief grating on azobenzene polymers analysis based on the fluid mechanics," *Mol Cryst Liq Cryst* vol. 345 pp. 587-592, 2000.
- [47] K. Sumaru, T. Yamanaka, T. Fukuda, and H. Matsuda, "Photoinduced surface relief gratings on azopolymer films analysis by a fluid mechanics model," *Appl Phys Lett* vol. 75 (13), pp. 1878-1880, 1999.
- [48] D. Bublitz, B. Fleck, and L. Wenke, "A model for surface relief formation in azobenzene polymers," *Appl Phys B Lasers*, vol. 72 (8), pp. 931-936, 2001.
- [49] D. Bublitz, M. Helgert, B. Fleck, L. Wenke, S. Hvilsted, and P. S. Ramanujam, "Photoinduced deformation of azobenzene polyester films," *Appl Phys B Lasers Opt* vol. 70 (6) pp. 863-865, 2000.
- [50] M. Saphiannikova, T. M. Geue, O. Henneberg, K. Morawetz, and U. Pietsch, "Linear viscoelastic analysis of formation and relaxation of azobenzene polymer gratings," *J Chem Phys* vol. 120 (8), pp. 4039-4045, 2004.
- [51] A. C. Mitus, G. Pawlik, A. Miniewicz, and F. Kajzar, "Kinetics of diffraction gratings in a polymer matrix containing azobenzene chromophores experiment and Monte Carlo simulations," *Mol Cryst Liq Cryst* vol. 416 pp. 113-126, 2004.
- [52] G. Pawlik, A. C. Mitus, A. Miniewicz, and F. Kajzar, "Kinetics of diffraction gratings formation in a polymer matrix containing azobenzene chromophores experiments and Monte Carlo simulations," *J Chem Phys* vol. 119 (13) pp. 6789-6801, 2003.
- [53] G. Pawlik, A. C. Mitus, A. Miniewicz, and F. Kajzar, "Monte Carlo simulations of temperature dependence of the kinetics of diffraction gratings formation in a polymer matrix containing azobenzene chromophores," *J Nonlinear Opt Phy Mater*, vol. 13(3-4), pp. 481-489, 2004.

- [54] P. Lefin, C. Fiorini, and J. M. Nunzi, "Anisotropy of the photo induced translation diffusion of azobenzene dyes in polymer matrices," *Pure Appl Opt* vol. 7 (1) pp. 71-82, 1998.
- [55] P. Lefin, C. Fiorini, and J. M. Nunzi, "Anisotropy of the photoinduced translation diffusion of azo dyes," *Opt Mater*, vol. 9 (1-4), pp. 323-328, 1998.
- [56] T. G. Pedersen and P. M. Johansen, "Mean field theory of photoinduced molecular reorientation in azobenzene liquid crystalline side chain polymers," *Phys Rev Lett* vol. 79 (13) pp. 2470-2473, 1997.
- [57] T. G. Pedersen, P. M. Johansen, N. C. R. Holme, P. S. Ramanujam, and S. Hvilsted, "Mean field theory of photoinduced formation of surface reliefs in side chain azobenzene polymers," *Phys Rev Lett* vol. 80 (1) pp. 89-92, 1998.
- [58] O. Baldus and S. J. Zilker, "Surface relief gratings in photoaddressable polymers generated by cw holography," *Appl Phys B Lasers Opt*, vol. 72 (4) pp. 425-427, 2001.
- [59] S. P. Bian, W. Liu, J. Williams, L. Samuelson, J. Kumar, and S. Tripathy, "Photoinduced surface relief grating on amorphous poly(4 phenylazo phenol) films," *Chem Mater* vol. 12 (6) pp. 1585-1590, 2000.
- [60] J. Kumar, L. Li, X. L. Jiang, D. Y. Kim, T. S. Lee, and S. Tripathy, "Gradient force: the mechanism for surface relief grating formation in azobenzene functionalized polymers" *Appl Phys Lett* vol. 72 (17) pp. 2096-2098, 1998.
- [61] N. K. Viswanathan, S. Balasubramanian, L. Li, S. K. Tripathy, and J. Kumar, "A detailed investigation of the polarization dependent surface relief grating formation process on azo polymer films," *Jpn J Appl Phys* vol. 38 (10) pp. 5928-5937, 1999.
- [62] K. Yang, S. Z. Yang, and J. Kumar, "Formation mechanism of surface relief structures on amorphous azopolymer films," *Phys Rev B* vol. 73 (16), p. 165204 2006.
- [63] A. Ashkin, "Optical trapping and manipulation of neutral particles using lasers," *Proc Natl Acad Sci USA* vol. 94 (10) pp. 4853-4860, 1997.
- [64] P. C. Chaumet and M. N. Vesperinas, "Time averaged total force on a dipolar sphere in an electromagnetic field," *Opt Lett* vol. 25 (15) pp. 1065-1067, 2000.
- [65] H. Ishitobi, M. Tanabe, Z. Sekkat, and S. Kawata, "The anisotropic nanomovement of azo-polymers " *Opt Express*, vol. 15 (2), pp. 652-659, 2007.
- [66] H. Hamanaka, K. Tanaka, A. Matsuda, and S. Iizima, "Reversible photo-induced volume changes in evaporated As₂S₃ and As₄Se₅Ge₁ films," *Solid State Commun.*, vol. 19, pp. 499-501, 1976.

AUTOR'S PUBLICATION LIST

SCI Publications:

1. **U.Gertners**, J.Teteris, Light intensity and its polarization relation to the photoinduced mass movement in thin layers of chalcogenide vitreous semiconductors, *Journal of Optoelectronics and Advanced Materials*, (November-December 2011), Vol. 13, No 11-12, pp. 1462-1466;
2. A.Gerbreders, J.Aleksejeva, **U.Gertners**, J.Teteris, The synthesis of different variants of azo-polyurethane polymers for optical recording, *Journal of Optoelectronics and Advanced Materials*, (November-December 2011), Vol. 13, No 11-12, pp. 1559-1562;
3. **U.Gertners**, J.Teteris, Surface relief formation in amorphous chalcogenide thin films during holographic recording, *Optical Materials*, 32 (8), (June 2010), 807-810;
4. **U.Gertners**, J.Teteris, Surface relief formation during holographic recording, *Journal of Optoelectronics and Advanced Materials*, 11 (12), (December 2009), 1963-1966.

Other Publications:

5. **U.Gertners**, Z.Gertnere, E.Potanina, J.Teteris, Optical-field induced volume- and surface-relief formation phenomenon in thin films of vitreous chalcogenide semiconductors, *Proc. of SPIE*, Vol.8836, (September 2013), 88360X;
6. **U.Gertners**, J.Teteris, Photo-induced Mass Transport in Thin Films of Amorphous As_2S_3 , *Physics Procedia*, Vol.44, (May 2013), 45 – 51;
7. J.Teteris, M.Reinfelde, J.Aleksejeva, **U.Gertners**, Optical field-induced mass transport in soft materials, *Physics Procedia*, Vol.44, (May 2013), 151 – 158;
8. **U.Gertners**, J.Teteris, The impact of light polarization on the direct relief forming processes in As_2S_3 thin films, *IOP Conf. Ser.: Mater. Sci. Eng.*, Vol.38, (August 2012), 012026;
9. J.Teteris, **U.Gertners**, Optical field-induced surface relief formation on chalcogenide and azo-benzene polymer films, *IOP Conf. Ser.: Mater. Sci. Eng.*, Vol.38, (August 2012), 012012;
10. **U.Gertners**, J.Teteris, Photo-induced Mass Transfer in Chalcogenides, *IOP Conf. Ser.: Mater. Sci. Eng.*, Vol.23, (June 2011),

- 012007;
11. J.Teteris, **U.Gertners**, M.Reinfelde, Photoinduced mass transfer in amorphous As_2S_3 films, *Physica Status Solidi (c)*, 8, (May 2011), 2780–2784;
 12. J.Teteris, J Aleksejeva, **U.Gertners**, Photoinduced mass transport in soft materials, *IOP Conf. Ser.: Mater. Sci. Eng.*, Vol.23, (June 2011), 012002.

PARTICIPATION IN CONFERENCES

1. **U. Gertners**, J. Teteris, Z. Gertnere, E. Potanina, Direct Light-Induced Surface Patterning in a-As₂S₃ Thin Films, Scientific Conference of Physics and Natural Sciences: Open Readings, Vilnius, Lithuania, March 19-21, 2014
2. **U. Gertners**, J. Teteris, Z. Gertnere, E. Potanina, Investigation of Several Techniques for Light Induced Surface Patterning, 5th International Conference on Radiation interaction with materials: fundamentals and applications, Kaunas, Lithuania, May 12-15, 2014
3. **U.Gertners**, J.Teteris, Gaismas inducētās izmaiņas amorfās As₂S₃ plānās kārtiņās, LU CFI 29.zinātn. konference, 20. – 22. februāris 2013
4. **U.Gertners**, J.Teteris, Optical-Field Induced Surface-Relief Formation Phenomenon in Thin Films of Vitreous Chalcogenide Semiconductors, International conference Functional materials and nanotechnologies (FMNT13), Tartu, Estonia, April 21-24, 2013
5. **U.Gertners**, J.Teteris, Optical-field Induced Surface-relief Modification in Amorphous As₂S₃ Films, 6th International Conference on Amorphous and Nanostructured Chalcogenides (ANC6), Brasov, Romania, June 24-28, 2013
6. **U.Gertners**, Z.Gertnere, E.Potanina, J.Teteris, Optical-field induced volume- and surface-relief formation phenomenon in thin films of vitreous chalcogenide semiconductors, SPIE Optics + Photonics 2013, San Diego, ASV, August 24-29, 2013.
7. **U.Gertners**, J.Teteris, The Impact of Light Polarization on the Direct Relief Forming Processes in As₂S₃ Thin Films, International conference Functional materials and nanotechnologies (FMNT12), Riga, Latvia, April 17-20, 2012, p.176
8. **U.Gertners**, J.Teteris, Photo-induced Mass Transfer in Thin Films of Amorphous As₂S₃, 10th International Conference Solid State Chemistry 2012 (SSC2012), Czech Republic, Pardubice, June 10-14, 2012, p.143
9. **U.Gertners**, J.Teteris, Photo-induced Mass Movement in Chalcogenide Vitreous Semiconductors and Its Direction Versus the Polarization, 16th edition of the International Conference on Solid Films and Surfaces (ICSFS12), Genoa, Italy, July 1-6, 2012, MonA-POM.22
10. **U.Gertners**, J.Teteris, Surface relief modulation phenomena by light induced interference, 18th International Symposium on Non-Oxide

and New Optical Glasses (ISNOG12), St. Malo, France, July 1-5, 2012, II-P31

11. **U.Gertners**, Foto-inducētā masas pārbīde halkogenīdos, LU CFI 27.zinātn. konference, 14. – 16. februāris 2011, 86.lpp.
12. **U.Gertners**, J.Teteris, Photo-induced Mass Transfer in Chalcogenides, Int. Conf. Functional materials and nanotechnologies (FM&NT2011), Latvia, Riga, April 5 – 8, 2011, p.110.;
13. J.Teteris, **U.Gertners**, Photoinduced Mass Transport in Soft Materials, Int. Conf. Functional materials and nanotechnologies (FM&NT2011), Latvia, Riga, April 5 – 8, 2011, p.62.;
14. **U.Gertners**, J.Teteris, Light intensity and Its Polarization Relation to the Photo-induced Mass Movement in Thin Layers of Chalcogenide Vitreous Semiconductors, 5th International Conference on Amorphous and Nanostructured Chalcogenides (ANC5), Magurele-Bucharest, Romania, June 26 – July 1, 2011, p.35.;
15. J.Teteris, J.Aleksejeva, **U.Gertners**, Photoinduced Mass Transport in Amorphous Chalcogenide and Organic Polymer Films, 24th International Conference on Amorphous and Nanocrystalline Semiconductors (ICANS24), Nara, Japan, August 21 – 26, 2011, p.38.;
16. **U.Gertners**, J.Aleksejeva, J.Teteris, Photo-induced Structural Transformations in Chalcogenide Vitreous Semiconductors, 24th International Conference on Amorphous and Nanocrystalline Semiconductors (ICANS24), Nara, Japan, August 21 – 26, 2011, p.143.;
17. **U.Gertners**, Direct Photo-induced Surface-relief Formation in Thin Layers of Chalcogenide Vitreous Semiconductors, The 13th International Conference – School: Advanced Materials and Technologies 2011, Lithuania, Palanga, August 27 – 31, 2011, p.46.
18. J.Teteris, **U.Gertners**, M.Reinfelde, Photoinduced Mass Transfer in Disordered Materials, 17th International Symposium on Non-Oxide and New Optical Glasses (XVII ISNOG), Ningbo, China, June 13 – 18, 2010;
19. **U.Gertners**, Surface Relief Modulation Phenomena by Light Induced Interference, 4th International Conference on Optical, Optoelectronic and Photonic Materials and Applications (ICOOPMA2010), Budapest, Hungary, August 15 – 18, 2010, p.230.;
20. J.Teteris, **U.Gertners**, M.Reinfelde, Photoinduced Mass Transfer in Soft Materials, 4th International Conference on Optical, Optoelectronic and Photonic Materials and Applications (ICOOPMA2010), Budapest, Hungary, August 15 – 18, 2010, p.204.;

ACKNOWLEDGEMENT

I am grateful to my scientific supervisor Dr. phys. Janis Teteris for valuable discussions and help in the doctoral thesis during the whole period of doctoral studies. Thanks to Laboratory of Surface Physics for opportunity to use their equipment.

I would like to express my sincere gratitude to my wife Zanda for her moral support over these years.

This work has been supported by the European Social Fund within the project «Support for Doctoral Studies at University of Latvia».



LATVIJAS
UNIVERSITĀTE
ANNO 1919